RESEARCH ARTICLE

Demembranated skeletal and cardiac fibers produce less force with altered cross-bridge kinetics in a mouse model for limb-girdle muscular dystrophy 2i

Axel J. Fenwick,^{1,2} Peter O. Awinda,^{1,2} Jacob A. Yarbrough-Jones,^{1,2} Jennifer A. Eldridge,^{1,2} Buel D. Rodgers,^{2,3} and ¹ Bertrand C. W. Tanner^{1,2}

¹Department of Integrative Physiology and Neuroscience, Washington State University, Pullman, Washington; ²Washington Center for Muscle Biology, Washington State University, Pullman, Washington; and ³AAVogen, Inc., Rockville, Maryland Submitted 24 December 2018; accepted in final form 14 May 2019

Fenwick AJ, Awinda PO, Yarbrough-Jones JA, Eldridge JA, Rodgers BD, Tanner BC. Demembranated skeletal and cardiac fibers produce less force with altered cross-bridge kinetics in a mouse model for limb-girdle muscular dystrophy 2i. Am J Physiol Cell Physiol 317: C226-C234, 2019. First published May 15, 2019; doi:10.1152/ajpcell.00524.2018.—Limb-girdle muscular dystrophy 2i (LGMD2i) is a dystroglycanopathy that compromises myofiber integrity and primarily reduces power output in limb muscles but can influence cardiac muscle as well. Previous studies of LGMD2i made use of a transgenic mouse model in which a proline-to-leucine (P448L) mutation in fukutin-related protein severely reduces glycosylation of α-dystroglycan. Muscle function is compromised in P448L mice in a manner similar to human patients with LGMD2i. In situ studies reported lower maximal twitch force and depressed force-velocity curves in medial gastrocnemius (MG) muscles from male P448L mice. Here, we measured Ca²⁺-activated force generation and cross-bridge kinetics in both demembranated MG fibers and papillary muscle strips from P448L mice. Maximal activated tension was 37% lower in MG fibers and 18% lower in papillary strips from P448L mice than controls. We also found slightly faster rates of cross-bridge recruitment and detachment in MG fibers from P448L than control mice. These increases in skeletal cross-bridge cycling could reduce the unitary force output from individual cross bridges by lowering the ratio of time spent in a force-bearing state to total cycle time. This suggests that the decreased force production in LGMD2i may be due (at least in part) to altered cross-bridge kinetics. This finding is notable, as the majority of studies germane to muscular dystrophies have focused on sarcolemma or whole muscle properties, whereas our findings suggest that the disease pathology is also influenced by potential downstream effects on cross-bridge behavior.

cross bridge; dystrophy; kinetics; limb-girdle; myosin

INTRODUCTION

The limb-girdle muscular dystrophies (LGMD) are a group of muscular dystrophies that cause weakness and atrophy primarily in limb muscles. One subclass of muscular dystrophy, LGMD2i, is a dystroglycanopathy caused by genetic aberrations in the fukutin-related protein (FKRP) gene. FKRP mutations compromise glycosylation of α -dystroglycan and destabilize the dystrophin-glycoprotein complex, resulting in reduced sarcolemma adhesion between the actin cytoskeleton and the extracellular matrix (9, 15, 25). LGMD2i primarily

Address for reprint requests and other correspondence: B. C. W. Tanner, Dept. of Integrative Physiology and Neuroscience, Washington State University, Pullman, WA 99164 (e-mail: bertrand.tanner@wsu.edu).

presents as weakness in proximal muscles and difficulties in ambulation, which become progressively worse with age. As the condition progresses, patients often experience difficulty breathing and reduced cardiac output as respiratory and heart muscles become involved, potentially resulting in illness or death from secondary disorders (18, 36, 42, 43, 45, 48, 49).

One of the most successful transgenic models for LGMD2i is a homozygous "knock-in" mouse line carrying a prolineto-leucine missense mutation at FKRP residue 448 (P448L) (9, 63). P448L mice survive significantly longer than other LGMD2i models, although they lack almost all functional glycosylation of α -dystroglycan in muscles and the brain (9). These mice also display characteristics that reflect those observed in patients with FKRP-related muscular dystrophies, including severe muscle necrosis and fibrosis, sarcolemma degradation, centralization of nuclei, and lower grip strength (9, 10, 37, 38, 50, 51, 62), and as is the case in humans, these phenotypical markers can emerge or become worse as the animal ages (3). Our previous in situ measurements of medial gastrocnemius (MG) from P448L mice revealed lower normalized maximal twitch force, tetanic force, and power, most of which were attributed to an increased contribution from passive elements (51). It is intriguing that male P448L mice also had slower maximal and optimal shortening velocities as measured using force-velocity curves, while the normalized rate of force development was faster. Such differences may be indicative of changes in cross-bridge cycling in the P448L dystrophic

We measured isometric steady-state force production and cross-bridge kinetics in single demembranated (skinned) MG fibers and papillary strips from adult P448L mice. The P448L mice used in this study were older than those used in our previous studies (~13 vs. 6-7 mo old) to allow the disease phenotype to robustly manifest and lessen the impact of agedependent disparities, such as left ventricle dysfunction (37). While cardiac function, along with other disease markers, of P448L mice worsens with age, peak cardiac dysfunction is reached by ~12 mo of age (3, 60). Along with providing precise control and manipulation of the intracellular ionic conditions, the use of demembranated tissue in these experiments also allowed us to isolate cross-bridge behavior from differences in sarcolemma adhesion or other membrane properties that are often associated with the LGMD2i phenotype. We found less force production and faster rates of cross-bridge recruitment and detachment in MG fibers from P448L than control mice. Papillary strips from P448L mice also produced less force, but this was not correlated with any significant changes in cross-bridge kinetics. Such novel results indicate that the functional deficit in skeletal and cardiac muscle of P448L mice, and possibly patients with LGMD2i, may not stem completely from compromised sarcolemma integrity, per se, but also may be due to compensatory changes in sarcomere contractile dynamics.

MATERIALS AND METHODS

Animal models. All procedures were approved by the Institutional Animal Care and Use Committee at Washington State University and complied with the National Institutes of Health *Guide for the Use and Care of Laboratory Animals*. C57BL/6 [wild-type (WT)] mice were bred in a colony at Washington State University using mice originally sourced from Simonsen Laboratories. P448L mice were also bred in a colony at Washington State University using congenic P448L mice originally sourced from Dr. Qi L. Lu (Carolinas Medical Center, Charlotte, NC) (9). Adult (66- to 73-wk-old) male mice were anesthetized by isoflurane inhalation (3% volume in 95% O₂-5% CO₂ flowing at 2 l/min), and hearts were immediately excised and placed in dissecting solution on ice. This was quickly followed by removal of both MG muscles to be used for histology and skinned-fiber protocols.

Cardiac and MG histology. Skeletal muscle samples were dissected whole and flash-frozen in isopentane at −140°C for 30 s and kept frozen at −80°C until sectioned in a cryostat (model CM1950, Leica). Heart samples were dissected and flash-frozen in blocks of optimal cutting temperature compound under the same conditions. Samples were sectioned at 10 μm thickness, placed on slides, and kept at −20°C until stained. Slides were fixed with 4% paraformaldehyde, stained with hematoxylin and eosin (H&E), and covered with positively charged glass coverslips (all sourced from VWR). Cardiac fibrosis (i.e., collagen content) was assessed using a hydroxyproline colorimetric assay (catalog no. K555-100, BioVision).

Solutions for skinned skeletal fibers and cardiac strips. Muscle mechanics solution concentrations were formulated by solving equations describing ionic equilibria according to Godt and Lindley (19). Dissecting solution consisted of 50 mM N,N-bis(2-hydroxyethyl)-2-aminoethane sulfonic acid (BES), 30.83 mM K propionate, 10 mM Na azide, 20 mM EGTA, 6.29 mM MgCl₂, 6.09 mM ATP, 1 mM DTT, 50 μM leupeptin, 275 μM Pefabloc, and 1 μM E-64. Dissecting solution for cardiac preparations also contained 20 mM 2,3-butanedione monoxime. Skinning solution consisted of dissecting solution with 1% (wt/vol) Triton X-100 and 50% (wt/vol) glycerol. Storage solution consisted of dissecting solution and 50% (wt/vol) glycerol. Relaxing solution (pCa 8.0) contained 20 mM BES, 5 mM EGTA, 5 mM MgATP, 1 mM Mg²⁺, 0.3 mM P_i, 35 mM phosphocreatine, and 300 U/ml creatine kinase, with ionic strength adjusted to 200 with Na methanesulfonate, pH 7.0 at 17°C. The composition of activating solution was the same as relaxing solution, with pCa 4.8. Solutions were made in a single batch and divided into aliquots for use in tissue from both P448L and WT mice.

Skinned MG preparation. After extraction, mouse MG muscles were divided into bundles of \sim 50 fibers each, skinned overnight at 4°C, and stored at -20°C using the solutions described above. Individual fibers were teased from the bundles using forceps, and each end was secured with an aluminum T-clip. Fibers (n=18) were mounted between a piezoelectric motor (model P841.10, Physik Instrumente, Auburn, MA) and a strain gauge (model AE801, Kronex, Walnut Creek, CA) in a chamber maintained at 17°C. This temperature was used to ensure tissue integrity throughout the experiment and avoid tension rundown. Fibers were lowered into a 30- μ l droplet of relaxing solution and stretched to a sarcomere length of 2.5 μ m as measured by digital Fourier transform (IonOptix, Milton, MA). The cross-sectional area of the fibers was calculated by measurement of the top and side width of the fiber under \times 100 magnification and calculation of the area as an

ellipse once sarcomere length was set. Fibers were then Ca²⁺-activated by titration of the relaxing solution (pCa 8.0) to pCa 4.8 with activating solution. To achieve pCa 4.8, the activating solution was exchanged multiple times (5 washes), which reasonably ensures maximal activation. Kinetic measurements were made via stochastic length perturbation analysis once steady-state force was achieved, indicating full activation. All fibers were kinetically characterized as fast-twitch fibers and had viscous modulus profiles that were shifted toward frequencies significantly faster than those of slow-twitch fibers (28, 61).

Skinned cardiac muscle preparation. After extraction, papillary muscles were dissected from the mouse hearts and pared to thin strips (~180 μ m diameter, 700 μ m long). Cardiac strips were skinned overnight at 4°C and stored at -20°C using the solutions described above. Strips (n=22) were secured on either end with aluminum T-clips and mounted between a piezoelectric motor (model P841.40, Physik Instrumente) and a strain gauge (model AE801, Kronex) in a chamber maintained at 17°C. Strips were lowered into a 30- μ l droplet of relaxing solution and stretched to a sarcomere length of 2.2 μ m as measured by digital Fourier transform (IonOptix). The cross-sectional area of the fibers was calculated by measurement of the top and side width of the fiber under \times 100 magnification and calculation of the area as an ellipse once sarcomere length was set. Strips were then Ca²⁺-activated by titration of the relaxing solution (pCa 8.0) to pCa 4.8 with activating solution.

Dynamic mechanical analysis. Stochastic length perturbations were applied for 60 s, as previously described (16, 55, 56), using an amplitude distribution with a standard deviation of 0.05% muscle length over the frequency range 0.5–250 Hz. Elastic and viscous moduli, $E(\omega)$ and $V(\omega)$, were measured as a function of angular frequency (ω) from the in-phase and out-of-phase portions of the tension response to the stochastic length perturbation. The complex modulus, $Y(\omega)$, was defined as $E(\omega) + iV(\omega)$, where $i = \sqrt{-1}$. Fitting Eq. 1 to the entire frequency range of modulus values provided estimates of six model parameters (A, k, B, $2\pi b$, C, and $2\pi c$).

$$Y(\omega) = A(i\omega)^k - B\left(\frac{i\omega}{2\pi b + i\omega}\right) + C\left(\frac{i\omega}{2\pi c + i\omega}\right)$$
(1)

where the A term reflects the viscoelastic mechanical response of passive, structural elements in the muscle and holds no enzymatic dependence. The parameter A represents the combined mechanical stress of the strip, while the parameter k describes the viscoelasticity of these passive elements, where k = 0 represents a purely elastic response and k = 1 is a purely viscous response (41, 46). The B and C terms reflect enzymatic cross-bridge cycling behavior that produces frequency-dependent shifts in the viscoelastic mechanical response during Ca²⁺-activated contraction. These B and C processes characterize work-producing (cross-bridge recruitment) and work-absorbing (cross-bridge detachment) muscle mechanics, respectively (7, 26, 27, 47). The parameters B and C represent the mechanical stress from the cross bridges, and the rate parameters $2\pi b$ and $2\pi c$ reflect crossbridge kinetics that are sensitive to biochemical perturbations affecting enzymatic activity, such as MgATP, MgADP, or P_i concentration (35). Molecular processes contributing to cross-bridge recruitment or force generation underlie the cross-bridge recruitment rate, $2\pi b$. Similarly, processes contributing to cross-bridge detachment or force decay underlie the cross-bridge detachment rate, $2\pi c$.

Statistical analysis. Values are means ± SE. Sequential quadratic programming methods in Matlab (version 7.9.0, Mathworks, Natick, MA) were used for constrained nonlinear least-squares fitting of Eq. 1 to moduli. Statistical analysis of experimental data was performed in SPSS (IBM Statistics, Chicago, IL), with a main effect of P448L mutation and incorporation of pCa and frequency as a repeated measure where appropriate. This approach matches data from the same MG or heart sample to provide more statistical power than a one-way ANOVA when multiple samples are analyzed from each muscle.

First-order autoregression was assumed for the covariance structure, and post hoc analyses were performed using least significant difference corrections where appropriate. Statistical significance is reported at P < 0.05.

RESULTS

Histological markers. Hematoxylin and eosin stains were used to assess fiber and nuclei morphology in MG tissue slices (Fig. 1). Number and placement of nuclei within the cell were quantified to determine whether the tissue contained markers for the disease phenotype. High levels of central nucleation are often associated with on-going muscle repair in response to disorder or damage (6, 17). At least one instance of nuclei centralization occurred in ~31% of MG fibers from P448L mice compared with 2% of fibers from WT controls (P =0.002; Fig. 1C). Similarly, 33% of all nuclei detected in P448L mice were centralized compared with only 3% in WT controls (P = 0.011; Fig. 1D). The disease phenotype was also assessed in cardiac tissue with hematoxylin and eosin stains (Fig. 2, A and B) and by comparing levels of fibrosis (Fig. 2C). Fibrosis in cardiac tissue was assessed using a hydroxyproline colorimetric assay to measure the amount of hydroxyproline (a common amino acid found exclusively in mammalian collagen) (2, 24). Hearts from P448L mice contained ~45% more hydroxyproline than hearts from WT mice (0.032 vs. 0.022 μ g/ μ l, P = 0.017; Fig. 2C), indicating increased fibrosis and confirming a dystrophic phenotype in the P448L model.

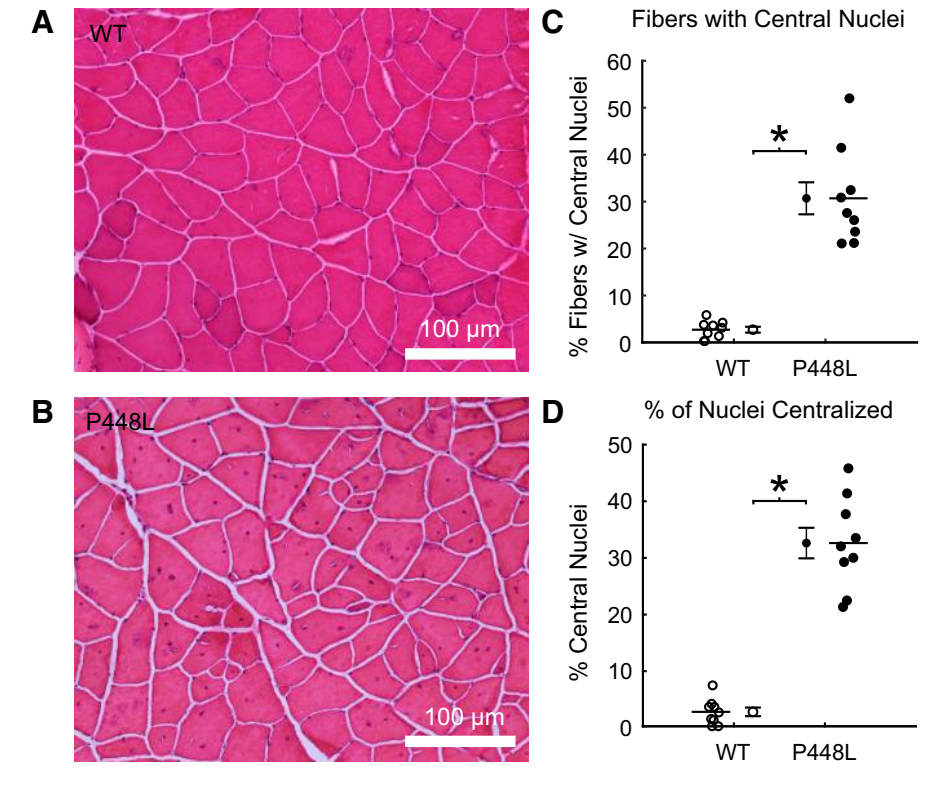
MG and papillary muscle force generation. Ca²⁺-activated tension was measured in permeabilized MG fibers by titration of Ca²⁺ from pCa 8.0 (relaxed) to pCa 4.8 (maximally activated) (Fig. 3A). Compared with WT controls, MG fibers from P448L mice produced 37% less tension during maximal activation (73.22 \pm 7.28 vs. 116.37 \pm 8.61 kN/m, P < 0.001),

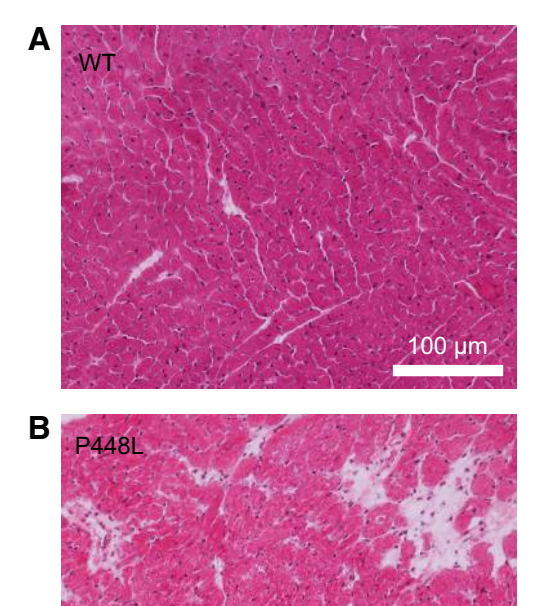
with significant differences at pCa <5.7. Tension values were fit to a three-parameter Hill curve, which showed no significant difference in Ca²⁺ sensitivity (pCa₅₀: 5.72 ± 0.02 vs. 5.71 ± 0.01 , P = 0.661) or cooperativity (Hill coefficient: 6.72 ± 1.29 vs. 6.17 ± 0.82 , P = 0.249). Passive tension was not significantly different between P448L and WT MG fibers (1.03 \pm 0.44 vs. 2.72 ± 0.84 kN/m²).

We also observed decreased tension in papillary muscles from P448L and WT mice (Fig. 3*B*). Maximal Ca²⁺-activated tension was 18% less in papillary strips from P448L than WT control mice (12.01 \pm 0.84 vs. 14.64 \pm 0.82 kN/m², *P* = 0.008), and tension values were consistently smaller at pCa <5.8. Papillary muscle strips from P448L mice were also less Ca²⁺-sensitive than those from WT mice (pCa₅₀: 5.55 \pm 0.04 vs. 5.63 \pm 0.03, *P* = 0.046). However, there were no significant differences in cooperativity (Hill coefficient: 5.73 \pm 0.31 vs. 6.69 \pm 0.49, *P* = 0.114) or passive tension (3.65 \pm 0.72 vs. 2.44 \pm 0.29 kN/m²) between the P448L and WT myocardium.

MG and papillary muscle kinetics. Modulus values (Fig. 4) were fit to Eq. 1 to solve for model parameters related to viscoelasticity (Eq. 1, A term), cross-bridge binding (Eq. 1, B and C terms), and cross-bridge kinetics (Eq. 1, $2\pi b$ and $2\pi c$) during full Ca²⁺ activation. There were no significant differences for parameters A, B, or C in permeabilized MG fibers between P448L mice and WT controls (Fig. 5, A, C, and E), indicating little change in viscoelastic stiffness or average number of cross bridges between groups. The value of k, which represents the viscoelastic stiffness of fibers, was smaller in fibers from P448L mice (Fig. 5B; 0.174 \pm 0.002 vs. 0.192 \pm 0.002, P < 0.001). This smaller k value suggests that fibers from P448L mice were slightly more elastic than those from WT mice. There were also kinetic differences between these groups for $2\pi b$ and $2\pi c$, which represent rates of cross-

Fig. 1. Medial gastrocnemius histology and nuclei quantification. A and B: sample H&E stains from medial gastrocnemius muscles from wild-type (WT) and P448L mice. Note the high level of central nucleation in fibers from P448L mice compared with WT controls. C: of all fibers counted, significantly more P448L fibers contained \geq 1 central nucleus. D: fraction of central nuclei vs. peripheral nuclei was greater for P448L fibers; peripheral nuclei predominate in healthy muscle cells. *P < 0.05 (by one-way ANOVA); 3 images from each tissue sample were averaged: n = 3 WT and 3 P448L mice.





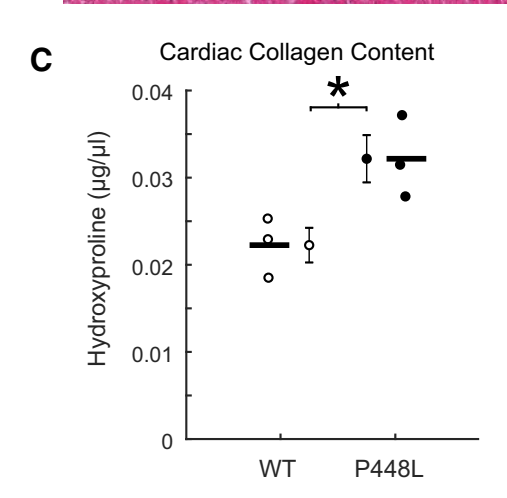


Fig. 2. Cardiac histology and collagen quantification. *A* and *B*: sample H&E stains from left ventricular wall tissue from wild-type (WT) and P448L mice. Note larger fibrotic areas in tissue from P448L mice. *C*: collagen content, as measured by hydroxyproline colorimetric assay, was significantly greater in homogenized heart tissue from P448L than WT mice. *P < 0.05 (by one-way ANOVA); n = 3 WT and 3 P448L hearts.

bridge recruitment and detachment, respectively. Cross-bridge recruitment rate was 7% faster (Fig. 5*D*; 115.23 \pm 2.89 vs. 106.81 \pm 2.14 s⁻¹, P = 0.029) and cross-bridge detachment rate was 8% faster (Fig. 5*F*; 130.56 \pm 2.51 vs. 119.82 \pm 2.14 s⁻¹, P = 0.005) for MG fibers from P448L than WT mice.

Modulus values from papillary strips were also fit to Eq. 1 to determine potential differences in myocardial viscoelastic stiffness and cross-bridge properties during full Ca²⁺ activation. As was the case in MG fibers, papillary strips did not show significant differences in parameters A, B, or C in strips from P448L mice compared with WT controls (Fig. 6, A, C, and E), indicating little change in viscoelastic stiffness or total cross-

bridge binding. Moreover, k was not significantly different between groups for these myocardial measurements (Fig. 6B; 0.191 ± 0.014 vs 0.213 ± 0.008 , P = 0.165). While crossbridge kinetics $(2\pi b$ and $2\pi c)$ appear to be trending toward faster recruitment and detachment rates in papillary strips from P448L than WT mice (similar to kinetic data for MG measurements), these differences were not significantly different between groups $[2\pi b: 81.02 \pm 10.11$ vs. 65.90 ± 6.07 s⁻¹, P = 0.185 (Fig. 6D); $2\pi c: 97.19 \pm 7.76$ vs. 88.03 ± 2.74 s⁻¹, P = 0.359 (Fig. 6F)].

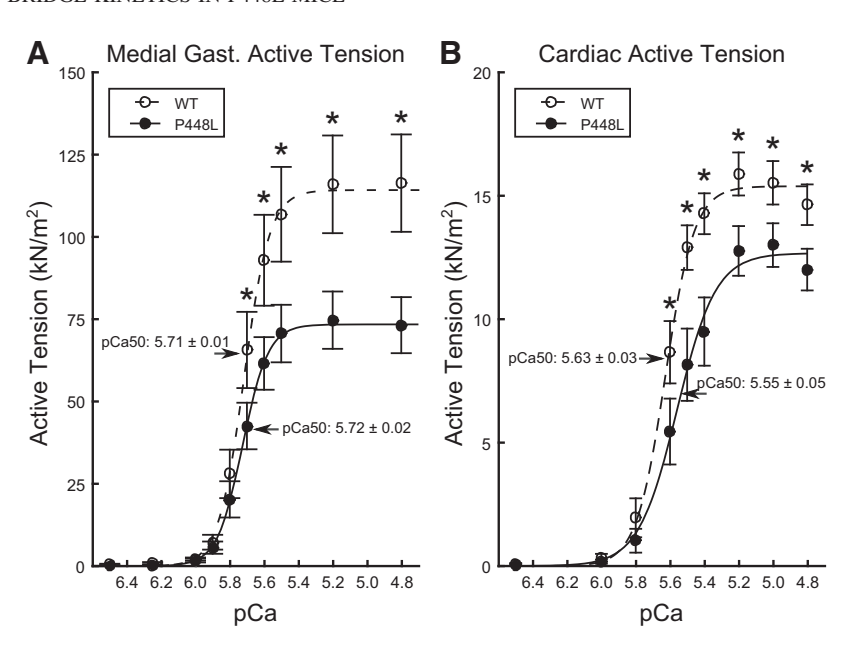
DISCUSSION

Muscular dystrophies impose clear and negative effects on patients, often involving muscle weakness that can severely impair ambulation or compromise cardiac and respiratory function. Precisely how the disorders alter function from the protein level to the whole muscle remains unclear. These diseases primarily result from mutations in proteins of the dystrophinglycoprotein complex and are, therefore, assumed to disrupt sarcolemma adhesion and regulation (32). In LGMD2i, mutations within the FKRP gene result in aberrant glycosylation of α-dystroglycan, destabilizing the complex. Force generated within the sarcomere must propagate from the myofibrils and fibers to the muscle bundle, and destabilization of these complexes may impede this process. In addition, abnormal Ca²⁺ regulation of the sarcomere by the dystrophin-glycoprotein complex may drive inefficient activation. Perhaps because the disease targets proteins associated with the sarcolemma and mechanical integrity, study of force generation and myofilament protein function within the sarcomere has been largely neglected.

The P448L mouse line generated by Chan et al. (9), which almost completely lacks functional glycosylation of α-dystroglycan, is a favorable model for studying LGMD2i. These mice show many phenotypes associated with LGMD2i, including poor ambulation, muscle necrosis and fibrosis, sarcolemma degradation, reduced exercise capacity, and cardiac contractile abnormalities, even while maintaining relatively long life spans (9, 10, 37, 38, 50, 51, 62). Our skeletal muscle histology showed that the MG muscles of P448L mice had significant central nucleation, referring to both the number of fibers with at least one central nucleus and the number of all nuclei that were centralized (Fig. 1). Central nucleation is prominent in many muscle disorders, including all forms of LGMD, and is usually a marker for ongoing myofibril repair (17, 45). While Chan et al. (9) reported a loss of α -dystroglycan glycosylation in P448L hearts as well, they did not observe pronounced dystrophic markers using hematoxylin-and-eosin and trichrome staining (9). However, we detected a significant increase in cardiac collagen content, which clearly indicates higher levels of fibrosis in the heart (Fig. 2). Together, these observations demonstrate dystrophic markers in both skeletal and cardiac tissue from P448L mice.

We used permeabilized tissue to assess motor protein kinetics and force production separate from sarcolemma properties. The intracellular ionic conditions within permeabilized tissue are also comparatively easy to control and manipulate, allowing us to bypass any potential deficiencies in Ca²⁺ regulation by the dystrophin-glycoprotein complex. Some patients with LGMD2i express a fiber type disproportion that is skewed

Fig. 3. Ca^{2+} -activated tension. Tension was measured in permeabilized medial gastrocnemius (MG) fibers and papillary strips as Ca^{2+} was titrated from relaxed (pCa 8.0) to fully activated (pCa 4.8) conditions. A: tension was significantly reduced in MG fibers from P448L mice at pCa <5.7. Hill fits to the tension-pCa relationship (solid and dashed lines) did not indicate changes in Ca^{2+} sensitivity or cooperativity. B: tension was significantly reduced in papillary muscle strips from P448L mice at pCa <5.6. Hill fits to the tension-pCa relationship indicate a slight decrease in Ca^{2+} sensitivity for P448L strips but no changes in cooperativity. *P < 0.05 (by one-way ANOVA); n = 18 (8 WT and 10 P448L) MG fibers and 22 (11 WT and 11 P448L) papillary strips from 6 (3 WT and 3 P448L) mice



toward slow-twitch type I fibers (30), but all permeabilized fibers used in our experiments were kinetically profiled as fast-twitch fibers. Despite being chemically demembranated, tissue from both the MG and the heart of P448L mice produced less Ca²⁺-activated force than WT controls (Fig. 3). These findings suggest that some properties of the dystrophic phenotype

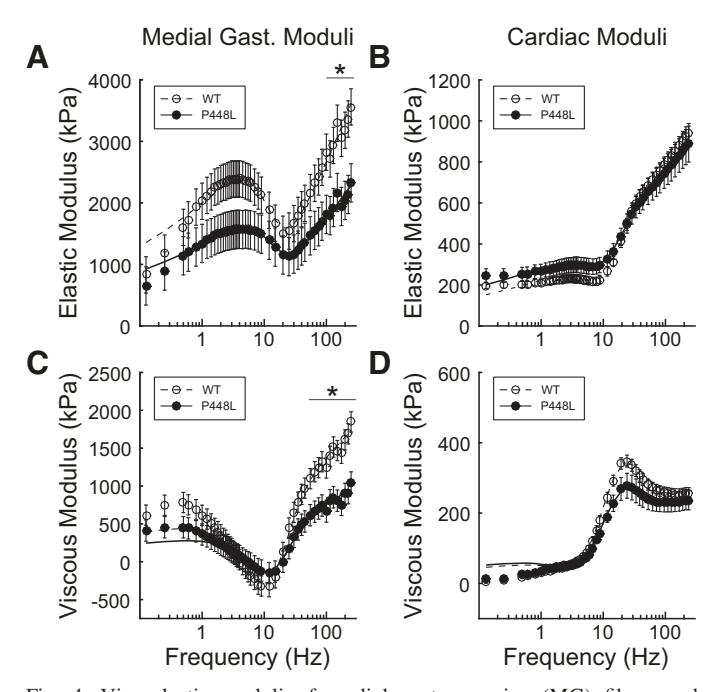


Fig. 4. Viscoelastic moduli of medial gastrocnemius (MG) fibers and papillary strips. Frequency-dependent elastic and viscous modulus values were measured by stochastic length perturbation analysis. A and C: elastic modulus magnitude of P448L MG fibers was significantly lower at perturbation frequencies >100 Hz, and viscous modulus magnitude was significantly lower at frequencies >45 Hz. B and D: there were no significant differences in elastic or viscous modulus magnitudes between P448L and WT papillary strips. *P < 0.05 (by one-way ANOVA); n = 18 (8 WT and 10 P448L) MG fibers and 22 (11 WT and 11 P448L) papillary strips from 6 (3 WT and 3 P448L) mice.

persist within the contractile framework of a fiber distinct from the mechanical stabilization and Ca²⁺ regulation of the sarco-lemma.

Dynamic mechanical analysis indicated that the rates of crossbridge recruitment and detachment are faster in MG fibers from P448L mice than WT controls, which could contribute to the decreased isometric steady-state force production we observed. Myosin detachment is the rate-limiting step of the cross-bridge cycle in muscle fibers (16, 53, 55), and a faster rate of detachment would reduce the time myosin spends in the actin-bound force-producing state by lowering the ratio of time spent in a force-bearing state to total cycle time. As isometric force within the fiber is considered to be the product of the unitary force of the cross bridge and the total number of attached cross bridges, a decrease in this unitary force would decrease isometric force within the fiber. Whether this is consistent with previous suggestions that potential changes in cross-bridge kinetics could explain the depressed force-velocity curves generated in situ by P448L MG muscles (51) is unclear. Slower maximal shortening velocity and depressed force-velocity curves in the in situ preparation might suggest slower, not faster, rates of cross-bridge cycling, although the scale of those measurements can only approximate cross-bridge behavior. This discrepancy suggests that the changes in cross-bridge cycling in our permeabilized single-fiber preparations may not directly underlie the force-velocity differences observed in in situ preparations. Instead, they likely contribute to decreased force production within single fibers, which then combine with other compounding factors across larger biological scales, such as fatty intrusion, fibrosis, or decreased sarcolemma adhesion. As active tension increases within the fiber, the influence of the these combinatory factors becomes more apparent, resulting in significant tension differences between P448L and wild-type tissue during moderate to maximal activation. Additionally, cross-bridge cycling during in situ force-velocity experiments will be influenced by changes in load, which our isometric single-fiber experiments do not recreate. However, our measurements do show that cross-bridge cycling kinetics are al-

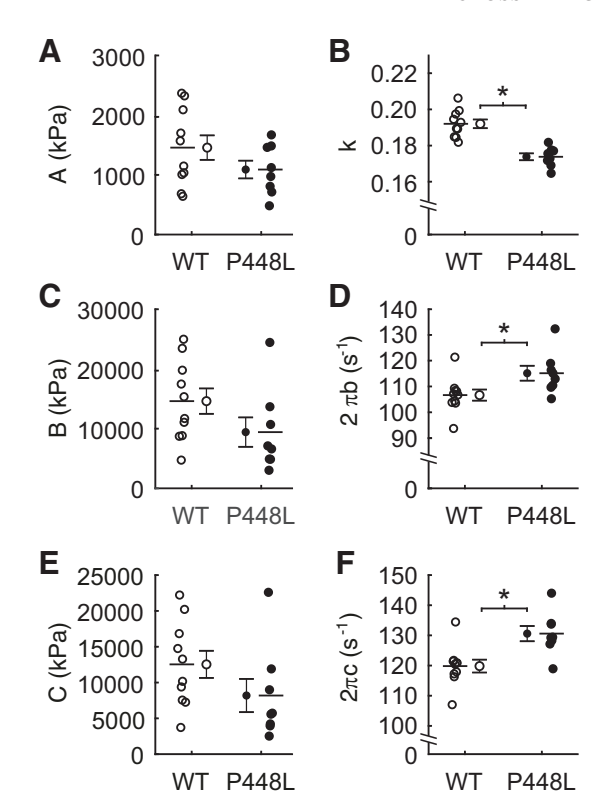


Fig. 5. Medial gastrocnemius (MG) parameter magnitudes and kinetics. Modulus values were fit to $Eq.\ 1$ to provide estimates of tissue viscoelasticity, cross-bridge binding, and cross-bridge kinetics. $A,\ C$, and E: no significant change was measured in parameters $A,\ B$, and C, respectively. B: parameter k, which describes viscoelasticity of passive elements of the tissue, was significantly lower in MG fibers from P448L than wild-type (WT) mice. D and F: kinetic parameters, $2\pi b$ and $2\pi c$, were faster in MG fibers from P448L mice, indicating faster rates of cross-bridge recruitment (D) and detachment (F). *P < 0.05 (by one-way ANOVA); n = 18 (8 WT and 10 P448L) MG fibers from 6 (3 WT and 3 P448L) mice.

tered in the P448L dystrophic model and suggest a potential mechanism whereby faster cross-bridge detachment rates could directly contribute to the decreased values of force generation observed here for MG fibers.

A specific accounting of the extent to which this force decrement can be linked to the increased rate of myosin recruitment and detachment rates, in combination, remains unclear. The chemical demembranation process provides reasonable assurance that the decreased force production must come from deficiencies within the myofilament proteins and, thus, is distinct from compromises to intermuscular or extracellular matrix properties typically considered with dystrophic myopathies. However, relatively few publications have probed the effects of muscular dystrophy on functional characteristics of single muscle fibers. In addition to the kinetic contributions to force decline we discussed above, it is important to consider additional potential contributors, for example, changes in protein expression or posttranslational modification of contractile proteins. However, although we did not observe differences in sarcomeric protein content or phosphorylation in MG tissue samples, relative phosphorylation of cardiac myosin-binding protein C (cMyBP-C) was slightly (~18%) lower in left ventricle tissue from P448L hearts (Supplemental Fig. S1 available at https://doi.org/10.6084/m9.figshare.8028911) (P = 0.023).

Higher levels of cMyBP-C phosphorylation are often correlated with increased tension, which is consistent with increased tension in WT compared with P448L cardiac strips (13, 31, 40). Decreased cMyBP-C phosphorylation via PKA has also been observed in muscular dystrophy in golden retrievers (1). Another possibility is that a decrease in myofibril density within the fiber could further reduce force output without proportionally decreasing the cross-sectional area. We were unable to assess myofibril density between the dystrophic and control mechanics fibers, which has also led us to focus on the kinetics differences that we observed between the two models and their correlation with force decreases. Given the intriguing and unique contributions to contractile dysfunction at the myofilament level that we present, this study represents only a starting point to further assess other contractile and regulatory differences at the molecular level in skeletal and cardiac muscle fibers from P448L mice and other models of muscular dystrophy.

Previous studies investigating the impact of muscular dystrophy on myosin kinetics frequently use samples from *mdx* mice, a model for Duchenne muscular dystrophy, although results have been inconclusive. In agreement with our findings, faster cross-bridge cycling was also observed in diaphragm muscle from *mdx* mice (11). These preparations exhibited shorter

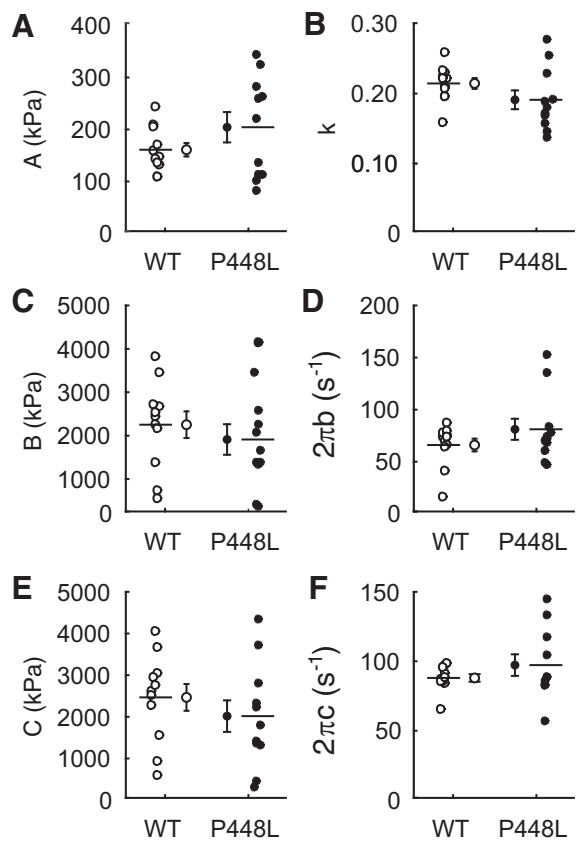


Fig. 6. Papillary muscle parameter magnitudes and kinetics. Modulus values were fit to $Eq.\ 1$ to provide estimates of tissue viscoelasticity, cross-bridge binding, and cross-bridge kinetics. $A,\ C$, and E: parameters $A,\ B$, and C, respectively. B: parameter $k.\ D$ and F: kinetic parameters, $2\pi b$ and $2\pi c$. No significant difference was measured in any of the 6 parameters between wild-type (WT) and P448L myocardial strips. Statistical significance was determined by one-way ANOVA; $n=22\ (11\ WT$ and $11\ P448L)$ papillary strips from 6 (3 WT and 3 P448L) mice.

cross-bridge duration (faster cycling), reduced force per cross bridge, and fewer cross bridges overall, which together reduced tension and increased ATPase activity. However, in vitro motility assays using purified myosin from *mdx* gastrocnemius muscle and diaphragm measured a slower actin sliding velocity (8, 12), although these experiments provide strong evidence that myosin function itself may be impaired in muscular dystrophy.

How disruption of the dystrophin-glycoprotein complex in muscular dystrophy would lead to changes in cross-bridge kinetics is not entirely clear. Damage to muscle tissue and downstream effects of muscular dystrophies can induce a variety of changes in the sarcomere environment, including increased proteolytic activity, altered Ca²⁺ regulation, and posttranslational modifications to myofilament proteins (21, 29, 39, 52, 54, 57-59). Turner et al. (59) found that intracellular free Ca²⁺ concentration was elevated skeletal fibers from mdx mice and that this Ca²⁺ flux caused an increase in protein degradation within the myofibrils. Dystrophic samples and mouse models are also especially prone to oxidative stress (5, 14, 22), which can influence sarcomere proteins, including myosin (20, 44). Fasttwitch skeletal muscle fibers appear to be disproportionately targeted in LGMD2i and many of the other muscular dystrophies. For instance, the in vitro motility assay, which detected slower actin sliding with purified type 2B myosin from mdx gastrocnemius, could not be reproduced with type 1 myosin from mdx soleus (8).

Cardiac function is often impaired both in human patients with LGMD2i (4, 18, 36, 43, 48, 49) and in P448L mice (3, 9, 37, 50). While we also observed decreased active tension in papillary strips from P448L mice, the rates of cross-bridge recruitment and detachment were not significantly different from WT controls. In this case, the decreased tension may stem primarily from the increased collagen content in the papillary tissue (Fig. 2), which would reduce the available contractile machinery for the same cross-sectional area of the experimental preparations. This impaired force production within the sarcomere could directly influence the tissue's ability to contract effectively, potentially resulting in dysfunction throughout the heart. In our previous study we assessed cardiac performance in P448L mice and found significant differences between P448L and WT mice. Systolic volume was roughly twofold higher in P448L females and accompanied by lower measures of fractional shortening, ejection fraction, and stroke volume (37). These differences could be the result of impaired force production within the tissue, although the root cause remains unclear. While our data indicate that cross-bridge kinetics are affected less in cardiac tissue, the low-impact lifestyle of the animals may have limited potential damage or downstream effects. The effect of exercise on muscular dystrophy remains unclear, but it is generally thought that lowimpact exercise may improve health and strengthen muscle but that high-intensity activities may cause further damage (23, 33, 34). Animals that are regularly exercised could therefore show exacerbated symptoms and more significant differences between WT and diseased animals. Further studies that include challenges to cardiac function, such as forced exercise, may reveal differences in cross-bridge kinetics that are clinically significant.

In summary, we show here that demembranated skeletal and cardiac tissues from a dystrophic mouse model produce less

active force and, in MG muscles, may be due in part to altered cross-bridge kinetics. Specifically, faster rates of cross-bridge recruitment and detachment may result in decreased overall force production and increased ATPase activity within the muscle. Our findings provide additional evidence that cross-bridge kinetics may be altered in some forms of muscular dystrophy, although the cause remains unclear. Further research is required to understand the full effect of the dystrophies on the contractile apparatus but may present a future target for drugs that influence the cross-bridge cycle to augment myosin force production.

ACKNOWLEDGMENTS

We thank Q. L. Lu for donating the mice that started the P448L breeding colony. We also thank Jim and Cindy Pru for help and advice with histological measurements.

GRANTS

These studies were supported by a grant from the Limb Girdle Muscular Dystrophy 2i Research Fund (to B. C. W. Tanner and B. D. Rodgers), American Heart Association Grant 17SDG33370153 (to B. C. W. Tanner), and National Science Foundation Grant 1656450 (to B. C. W. Tanner).

DISCLOSURES

B. D. Rodgers is the founder and chief executive officer of AAVogen, Inc. All other authors declare no competing interests.

AUTHOR CONTRIBUTIONS

A.J.F., B.D.R., and B.C.W.T. conceived and designed research; A.J.F., P.O.A., J.A.Y.-J., and J.A.E. performed experiments; A.J.F., P.O.A., J.A.Y.-J., and J.A.E. analyzed data; A.J.F., B.D.R., and B.C.W.T. interpreted results of experiments; A.J.F. prepared figures; A.J.F. drafted manuscript; A.J.F., B.D.R., and B.C.W.T. edited and revised manuscript; A.J.F., P.O.A., J.A.Y.-J., J.A.E., B.D.R., and B.C.W.T. approved final version of manuscript.

REFERENCES

- 1. Ait Mou Y, Lacampagne A, Irving T, Scheuermann V, Blot S, Ghaleh B, de Tombe PP, Cazorla O. Altered myofilament structure and function in dogs with Duchenne muscular dystrophy cardiomyopathy. *J Mol Cell Cardiol* 114: 345–353, 2018. doi:10.1016/j.yjmcc.2017.12.008.
- Berg RA, Prockop DJ. The thermal transition of a non-hydroxylated form of collagen. Evidence for a role for hydroxyproline in stabilizing the triple-helix of collagen. *Biochem Biophys Res Commun* 52: 115–120, 1973. doi:10.1016/ 0006-291X(73)90961-3.
- Blaeser A, Awano H, Wu B, Lu QL. Progressive dystrophic pathology in diaphragm and impairment of cardiac function in FKRP P448L mutant mice. PLoS One 11: e0164187, 2016. doi:10.1371/journal.pone.0164187.
- Boito CA, Melacini P, Vianello A, Prandini P, Gavassini BF, Bagattin A, Siciliano G, Angelini C, Pegoraro E. Clinical and molecular characterization of patients with limb-girdle muscular dystrophy type 2I. *Arch Neurol* 62: 1894–1899, 2005. doi:10.1001/archneur.62.12.1894.
- Brenman JE, Chao DS, Xia H, Aldape K, Bredt DS. Nitric oxide synthase complexed with dystrophin and absent from skeletal muscle sarcolemma in Duchenne muscular dystrophy. *Cell* 82: 743–752, 1995. doi:10.1016/0092-8674(95)90471-9.
- Cadot B, Gache V, Gomes ER. Moving and positioning the nucleus in skeletal muscle—one step at a time. *Nucleus* 6: 373–381, 2015. doi:10. 1080/19491034.2015.1090073.
- Campbell KB, Chandra M, Kirkpatrick RD, Slinker BK, Hunter WC. Interpreting cardiac muscle force-length dynamics using a novel functional model. Am J Physiol Heart Circ Physiol 286: H1535–H1545, 2004. doi:10. 1152/ajpheart.01029.2003.
- 8. Canepari M, Rossi R, Pansarasa O, Maffei M, Bottinelli R. Actin sliding velocity on pure myosin isoforms from dystrophic mouse muscles. *Muscle Nerve* 40: 249–256, 2009. doi:10.1002/mus.21302.
- Chan YM, Keramaris-Vrantsis E, Lidov HG, Norton JH, Zinchenko N, Gruber HE, Thresher R, Blake DJ, Ashar J, Rosenfeld J, Lu QL. Fukutin-related protein is essential for mouse muscle, brain and eye develop-

- ment and mutation recapitulates the wide clinical spectrums of dystroglycanopathies. *Hum Mol Genet* 19: 3995–4006, 2010. doi:10.1093/hmg/ddq314.
- Clement E, Mercuri E, Godfrey C, Smith J, Robb S, Kinali M, Straub V, Bushby K, Manzur A, Talim B, Cowan F, Quinlivan R, Klein A, Longman C, McWilliam R, Topaloglu H, Mein R, Abbs S, North K, Barkovich AJ, Rutherford M, Muntoni F. Brain involvement in muscular dystrophies with defective dystroglycan glycosylation. *Ann Neurol* 64: 573–582, 2008. doi:10.1002/ana.21482.
- Coirault C, Lambert F, Marchand-Adam S, Attal P, Chemla D, Lecarpentier Y. Myosin molecular motor dysfunction in dystrophic mouse diaphragm. *Am J Physiol Cell Physiol* 277: C1170–C1176, 1999. doi:10.1152/ajpcell.1999.277.6.C1170.
- Coirault C, Lambert F, Pourny J-CC, Lecarpentier Y. Velocity of actomyosin sliding in vitro is reduced in dystrophic mouse diaphragm. Am J Respir Crit Care Med 165: 250–253, 2002. doi:10.1164/ajrccm.165.2. 2105088
- Colson BA, Bekyarova T, Locher MR, Fitzsimons DP, Irving TC, Moss RL. Protein kinase A-mediated phosphorylation of cMyBP-C increases proximity of myosin heads to actin in resting myocardium. *Circ Res* 103: 244–251, 2008. doi:10.1161/CIRCRESAHA.108.178996.
- Disatnik M-H, Dhawan J, Yu Y, Beal MF, Whirl MM, Franco AA, Rando TA. Evidence of oxidative stress in mdx mouse muscle: studies of the pre-necrotic state. J Neurol Sci 161: 77–84, 1998. doi:10.1016/S0022-510X(98)00258-5.
- Ervasti JM, Campbell KP. A role for the dystrophin-glycoprotein complex as a transmembrane linker between laminin and actin. *J Cell Biol* 122: 809–823, 1993. doi:10.1083/jcb.122.4.809.
- Fenwick AJ, Leighton SR, Tanner BCW. Myosin MgADP release rate decreases as sarcomere length increases in skinned rat soleus muscle fibers. *Biophys J* 111: 2011–2023, 2016. doi:10.1016/j.bpj.2016.09.024.
- Folker ES, Baylies MK. Nuclear positioning in muscle development and disease. Front Physiol 4: 363, 2013. doi:10.3389/fphys.2013.00363.
- Godfrey C, Foley AR, Clement E, Muntoni F. Dystroglycanopathies: coming into focus. Curr Opin Genet Dev 21: 278–285, 2011. doi:10.1016/j.gde.2011.02.001.
- Godt RE, Lindley BD. Influence of temperature upon contractile activation and isometric force production in mechanically skinned muscle fibers of the frog. J Gen Physiol 80: 279–297, 1982. doi:10.1085/jgp.80.2.279.
- Gross SM, Lehman SL. Accessibility of myofilament cysteines and effects on ATPase depend on the activation state during exposure to oxidants. *PLoS One* 8: e69110, 2013. doi:10.1371/journal.pone.0069110.
- Guellich A, Negroni E, Decostre V, Demoule A, Coirault C. Altered crossbridge properties in skeletal muscle dystrophies. *Front Physiol* 5: 393, 2014. doi:10.3389/fphys.2014.00393.
- Haycock JW, Jones P, Harris JB, Mantle D. Differential susceptibility of human skeletal muscle proteins to free radical induced oxidative damage: a histochemical, immunocytochemical and electron microscopical study in vitro. *Acta Neuropathol* 92: 331–340, 1996. doi:10.1007/s004010050527.
- Hyzewicz J, Ruegg UT, Takeda S. Comparison of experimental protocols of physical exercise for *mdx* mice and Duchenne muscular dystrophy patients. *J Neuromuscul Dis* 2: 325–342, 2015. doi:10.3233/JND-150106.
- 24. de Jong S, van Veen TAB, de Bakker JMT, van Rijen HVM. Monitoring cardiac fibrosis: a technical challenge. Neth Heart J 20: 44–48, 2012. doi:10.1007/s12471-011-0226-x.
- Kanagawa M, Toda T. The genetic and molecular basis of muscular dystrophy: roles of cell-matrix linkage in the pathogenesis. *J Hum Genet* 51: 915–926, 2006. doi:10.1007/s10038-006-0056-7.
- 26. **Kawai M, Halvorson HR.** Two step mechanism of phosphate release and the mechanism of force generation in chemically skinned fibers of rabbit psoas muscle. *Biophys J* 59: 329–342, 1991. doi:10.1016/S0006-3495(91)
- 27. Kawai M, Wray JS, Zhao Y. The effect of lattice spacing change on cross-bridge kinetics in chemically skinned rabbit psoas muscle fibers. I. Proportionality between the lattice spacing and the fiber width. *Biophys J* 64: 187–196, 1993. doi:10.1016/S0006-3495(93)81356-0.
- 28. **Kawai M, Zhao Y.** Cross-bridge scheme and force per cross-bridge state in skinned rabbit psoas muscle fibers. *Biophys J* 65: 638–651, 1993. doi:10.1016/S0006-3495(93)81109-3.
- Kozakowska M, Pietraszek-Gremplewicz K, Jozkowicz A, Dulak J. The role of oxidative stress in skeletal muscle injury and regeneration: focus on antioxidant enzymes. *J Muscle Res Cell Motil* 36: 377–393, 2015. doi:10. 1007/s10974-015-9438-9.

- Krag TO, Hauerslev S, Sveen ML, Schwartz M, Vissing J. Level of muscle regeneration in limb-girdle muscular dystrophy type 2I relates to genotype and clinical severity. *Skelet Muscle* 1: 31, 2011. doi:10.1186/ 2044-5040-1-31.
- Kunst G, Kress KR, Gruen M, Uttenweiler D, Gautel M, Fink RHA.
 Myosin binding protein C, a phosphorylation-dependent force regulator in muscle that controls the attachment of myosin heads by its interaction with myosin S2. Circ Res 86: 51–58, 2000. doi:10.1161/01.RES.86.1.51.
- 32. **Lapidos KA, Kakkar R, McNally EM.** The dystrophin glycoprotein complex: signaling strength and integrity for the sarcolemma. *Circ Res* 94: 1023–1031, 2004. doi:10.1161/01.RES.0000126574.61061.25.
- Leung DG, Wagner KR. Therapeutic advances in muscular dystrophy. *Ann Neurol* 74: 404–411, 2013. doi:10.1002/ana.23989.
- 34. **Lovering RM, Brooks SV.** Eccentric exercise in aging and diseased skeletal muscle: good or bad? *J Appl Physiol* (1985) 116: 1439–1445, 2014. doi:10. 1152/japplphysiol.00174.2013.
- Lymn RW, Taylor EW. Mechanism of adenosine triphosphate hydrolysis by actomyosin. *Biochemistry* 10: 4617–4624, 1971. doi:10.1021/bi00801a004.
- Margeta M, Connolly AM, Winder TL, Pestronk A, Moore SA. Cardiac pathology exceeds skeletal muscle pathology in two cases of limbgirdle muscular dystrophy type 2I. *Muscle Nerve* 40: 883–889, 2009. doi:10. 1002/mus.21432.
- 37. Maricelli JW, Kagel DR, Bishaw YM, Nelson OL, Lin DC, Rodgers BD. Sexually dimorphic skeletal muscle and cardiac dysfunction in a mouse model of limb girdle muscular dystrophy 2i. *J Appl Physiol* (1985) 123: 1126–1138, 2017. doi:10.1152/japplphysiol.00287.2017.
- Maricelli JW, Lu QL, Lin DC, Rodgers BD. Trendelenburg-like gait, instability and altered step patterns in a mouse model for limb girdle muscular dystrophy 2i. *PLoS One* 11: e0161984, 2016. doi:10.1371/journal.pone.0161984.
- Monasky MM, Taglieri DM, Jacobson AK, Haizlip KM, Solaro RJ, Janssen PML. Post-translational modifications of myofilament proteins involved in length-dependent prolongation of relaxation in rabbit right ventricular myocardium. Arch Biochem Biophys 535: 22–29, 2013. doi: 10.1016/j.abb.2012.10.005.
- Moss RL, Fitzsimons DP, Ralphe JC. Cardiac MyBP-C regulates the rate and force of contraction in mammalian myocardium. *Circ Res* 116: 183–192, 2015. doi:10.1161/CIRCRESAHA.116.300561.
- Mulieri LA, Barnes W, Leavitt BJ, Ittleman FP, LeWinter MM, Alpert NR, Maughan DW. Alterations of myocardial dynamic stiffness implicating abnormal crossbridge function in human mitral regurgitation heart failure. Circ Res 90: 66–72, 2002. doi:10.1161/hh0102.103221.
- 42. **Muntoni F, Torelli S, Brockington M.** Muscular dystrophies due to glycosylation defects. *Neurotherapeutics* 5: 627–632, 2008. doi:10.1016/j.nurt.2008.08.005.
- Muntoni F, Torelli S, Wells DJ, Brown SC. Muscular dystrophies due to glycosylation defects: diagnosis and therapeutic strategies. *Curr Opin Neurol* 24: 437–442, 2011. doi:10.1097/WCO.0b013e32834a95e3.
- 44. Nogueira L, Figueiredo-Freitas C, Casimiro-Lopes G, Magdesian MH, Assreuy J, Sorenson MM. Myosin is reversibly inhibited by S-nitrosylation. Biochem J 424: 221–231, 2009. doi:10.1042/BJ20091144.
- 45. Norwood F, de Visser M, Eymard B, Lochmüller H, Bushby K; EFNS Guideline Task Force. EFNS guideline on diagnosis and management of limb girdle muscular dystrophies. *Eur J Neurol* 14: 1305–1312, 2007. doi:10.1111/j.1468-1331.2007.01979.x.
- 46. Palmer BM, Schmitt JP, Seidman CE, Seidman JG, Wang Y, Bell SP, Lewinter MM, Maughan DW. Elevated rates of force development and MgATP binding in F764L and S532P myosin mutations causing dilated cardiomyopathy. *J Mol Cell Cardiol* 57: 23–31, 2013. doi:10.1016/j. yjmcc.2012.12.022.
- 47. Palmer BM, Suzuki T, Wang Y, Barnes WD, Miller MS, Maughan DW. Two-state model of acto-myosin attachment-detachment predicts C-process of sinusoidal analysis. *Biophys J* 93: 760–769, 2007. doi: 10.1529/biophysj.106.101626.
- 48. Petri H, Sveen ML, Thune JJ, Vissing C, Dahlqvist JR, Witting N, Bundgaard H, Køber L, Vissing J. Progression of cardiac involvement in patients with limb-girdle type 2 and Becker muscular dystrophies: a 9-year follow-up study. *Int J Cardiol* 182: 403–411, 2015. doi:10.1016/j. ijcard.2014.12.090.
- 49. Poppe M, Cree L, Bourke J, Eagle M, Anderson LVB, Birchall D, Brockington M, Buddles M, Busby M, Muntoni F, Wills A, Busbby K. The phenotype of limb-girdle muscular dystrophy type 2I. *Neurology* 60: 1246–1251, 2003. doi:10.1212/01.WNL.0000058902.88181.3D.

- 50. Qiao C, Wang CH, Zhao C, Lu P, Awano H, Xiao B, Li J, Yuan Z, Dai Y, Martin CB, Li J, Lu Q, Xiao X. Muscle and heart function restoration in a limb girdle muscular dystrophy 2I (LGMD2I) mouse model by systemic FKRP gene delivery. *Mol Ther* 22: 1890–1899, 2014. doi:10.1038/mt.2014.141.
- 51. **Rehwaldt JD, Rodgers BD, Lin DC.** Skeletal muscle contractile properties in a novel murine model for limb girdle muscular dystrophy 2i. *J Appl Physiol* (1985) 123: 1698–1707, 2017. doi:10.1152/japplphysiol.00744.2016.
- Sander M, Chavoshan B, Harris SA, Iannaccone ST, Stull JT, Thomas GD, Victor RG. Functional muscle ischemia in neuronal nitric oxide synthase-deficient skeletal muscle of children with Duchenne muscular dystrophy. *Proc Natl Acad Sci USA* 97: 13818–13823, 2000. doi:10.1073/ pnas.250379497.
- 53. Siemankowski RF, Wiseman MO, White HD. ADP dissociation from actomyosin subfragment 1 is sufficiently slow to limit the unloaded shortening velocity in vertebrate muscle. *Proc Natl Acad Sci USA* 82: 658–662, 1985. doi:10.1073/pnas.82.3.658.
- Sumandea MP, Steinberg SF. Redox signaling and cardiac sarcomeres.
 J Biol Chem 286: 9921–9927, 2011. doi:10.1074/jbc.R110.175489.
- Tanner BCW, Breithaupt JJ, Awinda PO. Myosin MgADP release rate decreases at longer sarcomere length to prolong myosin attachment time in skinned rat myocardium. Am J Physiol Heart Circ Physiol 309: H2087– H2097, 2015. doi:10.1152/ajpheart.00555.2015.
- 56. Tanner BCW, Wang Y, Maughan DW, Palmer BM. Measuring myosin cross-bridge attachment time in activated muscle fibers using stochastic vs. sinusoidal length perturbation analysis. *J Appl Physiol* (1985) 110: 1101–1108, 2011. doi:10.1152/japplphysiol.00800.2010.

- Tidball JG, Wehling-Henricks M. Evolving therapeutic strategies for Duchenne muscular dystrophy: targeting downstream events. *Pediatr Res* 56: 831–841, 2004. doi:10.1203/01.PDR.0000145578.01985.D0.
- 58. **Tidball JG, Wehling-Henricks M.** The role of free radicals in the pathophysiology of muscular dystrophy. *J Appl Physiol* (1985) 102: 1677–1686, 2007. doi:10.1152/japplphysiol.01145.2006.
- Turner PR, Westwood T, Regen CM, Steinhardt RA. Increased protein degradation results from elevated free calcium levels found in muscle from mdx mice. Nature 335: 735–738, 1988. doi:10.1038/335735a0
- Vannoy CH, Xiao W, Lu P, Xiao X, Lu QL. Efficacy of gene therapy is dependent on disease progression in dystrophic mice with mutations in the FKRP gene. *Mol Ther Methods Clin Dev* 5: 31–42, 2017. doi:10.1016/j.omtm.2017.02.002.
- 61. **Wang G, Kawai M.** Force generation and phosphate release steps in skinned rabbit soleus slow-twitch muscle fibers. *Biophys J* 73: 878–894, 1997. doi:10.1016/S0006-3495(97)78121-9.
- 62. Willis TA, Hollingsworth KG, Coombs A, Sveen ML, Andersen S, Stojkovic T, Eagle M, Mayhew A, de Sousa PL, Dewar L, Morrow JM, Sinclair CDJ, Thornton JS, Bushby K, Lochmüller H, Hanna MG, Hogrel JY, Carlier PG, Vissing J, Straub V. Quantitative muscle MRI as an assessment tool for monitoring disease progression in LGMD2I: a multicentre longitudinal study. PLoS One 8: e70993, 2013. doi:10.1371/journal.pone.0070993.
- 63. Xu L, Lu PJ, Wang CH, Keramaris E, Qiao C, Xiao B, Blake DJ, Xiao X, Lu QL. Adeno-associated virus 9 mediated FKRP gene therapy restores functional glycosylation of α-dystroglycan and improves muscle functions. *Mol Ther* 21: 1832–1840, 2013. doi:10.1038/mt.2013.156.

